

## TURBULENT HEAT- AND-MASS-TRANSFER MODEL IN A NEAR-WALL ZONE OF SEPARATED FLOWS

A. V. Gorin and D. F. Sikovskii

UDC 532.526

**Introduction.** Modeling of turbulence and the processes of heat transfer in separated flows is an important problem of modern thermohydrodynamics. The main difficulty of this task is that of simulating adequately flow in near-wall zones, which play a determining part in heat transfer processes. In developed turbulent flow, the viscous sublayer, which usually accumulates the main thermal resistance, is very thin (comparable in order of magnitude with the Kolmogorov length scale). Numerical solution requires a high grid resolution near the boundary, which complicates the computation scheme and increases computer time.

To eliminate this difficulty, instead of flow calculation in the entire flow region up to the boundary, one should employ the condition of matching of the numerical solution with the so-called wall functions [1]

$$u_+ = \frac{1}{\alpha} \ln y_+ + B; \quad (1)$$

$$T_+ = \frac{1}{\alpha_t} \ln y_+ + B_t. \quad (2)$$

Here  $u_+ = u/v_*$ ;  $u$  is the longitudinal mean velocity;  $v_*$  is the friction velocity;  $T_+ = \rho c_0 v_* (T_w - T)/q$ ;  $T$  is the mean temperature;  $T_w$  is the wall temperature;  $q$  is the wall heat flux;  $\rho$  and  $c_0$  are the density and specific heat capacity;  $y_+ = v_* y/\nu$ ;  $y$  is the distance to the wall;  $\alpha$  and  $B$  are constants that are considered universal;  $\alpha_t$  and  $B_t$  are functions of the Prandtl number  $Pr = \nu/a$ ; and  $a$  is the thermal diffusivity.

The use of wall functions (1) and (2) is based on the hypothesis that boundary-layer turbulence has universal properties which are determined by the wall shear stress divided by density (an incompressible fluid is considered):  $\tau_w = v_*^2$ . However, violation of the universality of the logarithmic law of the wall in a turbulent boundary layer with an adverse pressure gradient  $dP/dx > 0$  was recently proved experimentally [2, 3]. In [3], a logarithmic section of the velocity profile (1) occurred near the wall; however, the quantity  $B$  decreased monotonically as the pressure gradient parameter  $P_+ = \nu(dP/dx)/(\rho v_*^3)$  increased; the value of  $\alpha$  varied slightly.

In earlier experiments of [2] with a wall shear stress (measured independently by an electrochemical technique), the turbulent boundary layer in a diffuser in the presence of separation was studied. As the separation cross-section was approached, despite a decrease in  $P_+$ , the value of  $B$  in law (1) decreased, while  $\alpha$  increased. Also, an ambiguity in the dependence of  $\alpha$  and  $B$  on  $P_+$  was observed: for similar values of  $P_+$ , the velocity profiles in the coordinates of the wall law  $u_+(y_+)$  differed significantly from each other.

Such boundary-layer behavior cannot be explained on the basis of traditional concepts, according to which the turbulence structure in the near-wall layer is determined only by the parameters in the averaged equations of motion. The nature of turbulent separating flow is much more complicated.

As compared with a zero-pressure-gradient boundary layer, an increase in turbulence intensity by more than a factor of two is observed (in the experiments of [2] the ratio of root-mean-square fluctuation amplitude of the longitudinal velocity  $u'$  to the mean local velocity  $u$  reached 0.7). Qualitative changes in the structure of Reynolds stresses, which involved an increase in the contribution of strong fluctuation events of  $u'v'$ , occurred near the separation.

---

Institute of Thermal Physics, Siberian Division, Russian Academy of Sciences, Novosibirsk 630090.  
Translated from *Prikladnaya Mekhanika i Tekhnicheskaya Fizika*, Vol. 37, No. 3, pp. 83–96, May–June, 1996.  
Original article submitted December 16, 1994; revision submitted March 15, 1995.

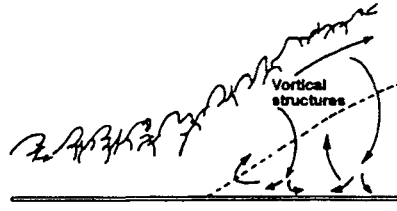


Fig. 1

Simpson [4] noted the significant role of large-scale coherent structures in separated turbulent flow, which results in an unsteady separation process. Unsteadiness is most pronounced at the separation point and in the backflow zone. Backflow is initiated by large vortex structures which arrive from the mixing layer above the recirculation zone. The turbulence intensity in this region is on the order of unity and even higher in some places [4–6]. Simpson [4] concluded that the mean velocity profile in backflow is the result of time averaging of unsteady turbulent flow of large amplitude and large space scale, and, therefore, the Reynolds shear stress has no local connection with the average velocity gradient. Thus, information only on the mean flow parameters is not sufficient to simulate adequately separating turbulent flows. One should also use the fluctuation characteristics related to unsteady separation.

We propose a physical model of near-wall turbulent separated flow that is based on the assumption of the governing role of the induced local pressure gradient  $\alpha_{rms}$  in transfer processes that take place in the close proximity of the wall in separated flow. This assumption is related to the idea (based on experimental observations) that flow in the near-wall zone is subjected to intense instantaneous accelerations induced by large-scale vortex flow structures. The root-mean-square wall-pressure gradient  $\alpha_{rms}$  is a qualitative characteristic of these accelerations. From considerations of similitude and dimensionality, we derive laws for the behavior of the mean and fluctuating characteristics of near-wall turbulence, velocity and pressure fluctuation spectra, the “2/3 power law” ( $Nu \sim Re^{2/3}$ ) for the wall heat-and-mass-transfer coefficient, and the relationship between the latter and the pressure fluctuation level on the wall  $h \sim (p'_{rms})^{1/3}$ . The laws obtained are confirmed by the available experimental data.

**Turbulence Structure in the Boundary Layer of Separated Flows.** Before considering the principles of the model proposed here, we cite some known experimental data for separated flow on a flat surface studied in [7].

In the recirculation zone behind the separation point, the backflow velocity has a maximum  $U_N$  at a distance  $N$  from the wall which is far smaller than the local boundary layer thickness  $\delta$  [the distance from the wall at which the longitudinal velocity  $U$  becomes  $0.99U_\infty$  ( $U_\infty$  is the external flow velocity in the given cross-section)]. In the cross section  $x = 397.3$  cm, we have  $N = 0.06\delta$ . The flow region of  $0 < y < N$  is usually called the near-wall zone of recirculation flow.

Let us estimate the scales of turbulent motion in the near-wall zone. According to the measurement results of [7] for longitudinal velocity spectra, the characteristic frequency of large-scale motion is

$$f \sim 5 \cdot 10^{-2} U_\infty / \delta. \quad (3)$$

Assuming that the phase velocity of turbulent disturbances is of the order of  $U_N$ , with allowance for (3), we obtain an estimate of the wavelength

$$\lambda \sim U_N / f \sim 20\delta U_N / U_\infty \sim 2\delta, \quad (4)$$

since the ratio  $U_N / U_\infty$  is on the order of  $10^{-1}$  [7]. With allowance for of the estimate  $N \sim 0.06\delta$ , relation (4) can be written as

$$\lambda / N \sim 33. \quad (5)$$

Thus, the spatial dimensions of low-frequency fluctuations of the longitudinal velocity in the near-wall layer are much greater than the layer thickness. On the other hand, according to the measurements of [7], the

root-mean-square fluctuation of the transverse velocity  $v'_{rms}$  in the near-wall layer is an order of magnitude lower than the longitudinal fluctuation  $u'_{rms}$ . These facts indicate that the large-scale motion in the near-wall layer is of the character of an unsteady boundary layer. In this case the role of external flow is played by large-scale unsteady recirculation flow supported by large-scale vortices from the mixing layer above (see Fig. 1, where the dashed curve represents zero velocity). Since the fluctuation level  $u'_{rms}$  is on the order of the mean velocity  $U$ , unsteady motion in the boundary layer is characterized by a large amplitude. Reasoning from (3)–(5) and the above data, the characteristic frequency is related to the boundary layer parameters by the estimate

$$f \sim 3 \cdot 10^{-2} U_N / N. \quad (6)$$

Thus, turbulent motion in the boundary layer can be divided into two components: a large-scale component with a length scale much greater than the near-wall layer thickness  $N$  and a small-scale component, which is composed of vortices with a size of the order of  $N$  and smaller. Averaging the Navier–Stokes equations over small-scale fluctuations and assuming no correlation between large-scale and small-scale velocity fluctuations, we obtain the equations of large-scale motion in the near-wall layer in a boundary-layer approximation:

$$\frac{\partial \mathbf{u}}{\partial t} + u \frac{\partial \mathbf{u}}{\partial x} + w \frac{\partial \mathbf{u}}{\partial z} + v \frac{\partial \mathbf{u}}{\partial y} + \alpha = \frac{\partial \tau}{\partial y} + \nu \frac{\partial^2 \mathbf{u}}{\partial y^2}, \quad \frac{\partial u}{\partial x} + \frac{\partial v}{\partial y} + \frac{\partial w}{\partial z} = 0. \quad (7)$$

Here  $\mathbf{u} = (u, w)$  is the large-scale velocity vector;  $u$ ,  $w$ , and  $v$  are the  $x$ ,  $z$ , and  $y$  velocity components;  $\alpha = \rho^{-1} (\partial p / \partial x, \partial p / \partial z)$  is the large-scale kinematic pressure gradient;  $\tau = -(\langle u'v' \rangle, \langle v'w' \rangle)$  is the large-scale Reynolds stress; the angle brackets denote averaging over small-scale fluctuations; the  $Ox$  axis is directed along the free flow; and the prime denotes small-scale velocity fluctuations. Equation (7) takes into account the three-dimensionality of large-scale motion in the separated flow.

In deriving the unsteady Reynolds equations (7), we applied the Reynolds averaging rules [8]:

$$\langle \Psi' \rangle = \langle \Phi' \rangle = 0, \quad \langle \Phi \Psi \rangle = \langle \Phi \rangle \langle \Psi \rangle + \langle \Phi' \Psi' \rangle, \quad \langle \Phi' \langle \Phi \rangle \rangle = \langle \Psi' \langle \Psi \rangle \rangle = 0$$

where  $\Phi$  and  $\Psi$  are variables related to the flow (pressure or any velocity component).

The boundary layer described by Eqs. (7) has a time-dependent thickness  $\delta_N(t, x, z)$ , whose average over a large time interval equals  $N(x)$ . For  $y = \delta_N$ , the velocity field  $\mathbf{u}$  should match the external large-scale velocity field  $\mathbf{U}_e(t, x, z)$ , and the Reynolds stresses should match the external large-scale field  $\tau_e(t, x, z)$ :

$$\mathbf{u} = \mathbf{U}_e, \quad \tau = \tau_e \quad \text{at} \quad y = \delta_N. \quad (8)$$

The conditions of attachment and vanishing of turbulent stresses are assigned at the wall ( $y = 0$ ):

$$\mathbf{u} = 0, \quad \tau = 0 \quad \text{at} \quad y = 0. \quad (9)$$

When the distances from the wall are far smaller than the near-wall layer thickness, convective terms in Eq. (7) are insignificant, and the equation of motion expresses the balance between the pressure gradient and the Reynolds and viscous stresses:

$$\alpha = \frac{\partial \tau}{\partial y} + \nu \frac{\partial^2 \mathbf{u}}{\partial y^2}, \quad y \ll \delta_N.$$

Integrating with respect to  $y$ , with allowance for (9), we obtain

$$\tau = \tau_w + \alpha y - \nu \frac{\partial \mathbf{u}}{\partial y}, \quad (10)$$

where  $\tau_w = \nu (\partial \mathbf{u} / \partial y)_{y=0}$  is the wall shear stress.

When the Reynolds numbers of the free flow are fairly great, a viscous sublayer is in the proximity of the wall. The sublayer thickness is far less than the boundary layer thickness ( $l_v \ll \delta_N$ ). For  $y \gg l_v$ , viscosity affects only slightly the Reynolds stress distribution, the last term in (10) can be ignored, and we have

$$\tau = \tau_w + \alpha y, \quad l_v \ll y \ll \delta_N. \quad (11)$$

In steady zero-pressure-gradient flow ( $\partial u/\partial t = 0$ ,  $\alpha = 0$ ) expression (11) is of the form  $\tau = \tau_w$ , which corresponds to a sublayer of constant shear stress, within which the statistical characteristics of turbulence are determined by the friction velocity  $v_*$ .

As was noted above, in the presence of a pressure gradient, a sublayer of constant shear stress exists only for sufficiently small values of  $P_+$ . The critical value of  $P_+$ , beginning from which the sublayer disappears, can be estimated as follows. It is known that a logarithmic velocity profile characteristic of the constant-stress sublayer occurs in zero-pressure-gradient flow when  $y > 30\nu/v_*$ . On the other hand, following (11), when  $y \sim v_*^2/\alpha$ , the effect of the pressure gradient on the Reynolds shear stress distribution near the wall becomes significant. Thus, one can assume that for  $v_*^2/\alpha \sim 30\nu/v_*$ , i.e., for  $P_+ \sim 3 \cdot 10^{-2}$ , the effect of the pressure gradient reaches the boundaries of the viscous sublayer, and the constant-stress sublayer degenerates. This estimate agrees with the experimental results of [2], which showed the absence of a logarithmic wall law for  $P_+ \sim 2 \cdot 10^{-2}$ .

In separated flows the instantaneous values of  $P_+$  can exceed significantly the above value. For separated flow behind a backward facing step of height  $H$ , one can write the following estimates for the orders of instantaneous values of  $\alpha$  and  $\tau_w$ :

$$\alpha \sim p'/(\rho H) = C_{p'} U_\infty^2/(2H); \quad (12)$$

$$\tau_w \sim \tau'_w = C_f U_\infty^2/2. \quad (13)$$

Here  $p'$  and  $\tau'_w$  are the root-mean-square fluctuations of pressure and wall shear stress. By virtue of (12) and (13), we obtain

$$P_+ = \nu\alpha/(\tau_w)^{3/2} \sim 2^{1/2} C_{p'}/(\text{Re}_H C_f^{3/2}). \quad (14)$$

The typical value of  $C_{p'}$  in separated flows is  $10^{-1}$  [9]. For separated flows [6],  $C_{f',\text{max}} = 8 \cdot 10^{-4}$  for  $\text{Re}_H = 3.5 \cdot 10^4$  in the vicinity of the reattachment point. Substituting these values into (14), we have  $P_+ \sim 2 \cdot 10^{-1}$ , which exceeds by an order the critical value found above.

Thus, fluid acceleration in the near-wall layer that is produced by large-scale vortices of separated flows prevents formation of a sublayer of constant shear stress. In this connection, the friction velocity  $v_*$  is not a governing parameter of the near-wall layer of turbulent separated flow. Following (11), the governing parameter is an instantaneous value of the kinematic pressure gradient  $\alpha$ :

$$\tau = \alpha y, \quad l_v \ll y \ll \delta_N, \quad (15)$$

because  $\tau_w$  in (11) can be ignored compared with  $\alpha y$ . The statistical regime of turbulent flow in the region of  $l_v \ll y \ll \delta_N$  should be determined by the only parameters of the problem:  $\alpha$  and  $y$ . Then, from dimensionality considerations, the thickness of the viscous sublayer is given by

$$l_v \sim \nu^{2/3} \alpha^{-1/3} \quad (\alpha = |\alpha|). \quad (16)$$

For the mean velocity profile, one can write

$$\frac{\partial \mathbf{u}}{\partial y} = \frac{1}{\varkappa} \frac{\alpha}{\alpha} \left( \frac{\alpha}{y} \right)^{1/2} \quad (17)$$

( $\varkappa$  is a universal constant). In projection onto  $\alpha$ , formulas (15) and (17) lead to the well-known Prandtl formula  $\tau = (\varkappa y du/dy)^2$ . Integration of (17) with respect to  $y$  gives a "half-power law" for the large-scale longitudinal velocity profile:

$$\mathbf{u} = \frac{2}{\varkappa} \frac{\alpha}{\alpha} (\alpha y)^{1/2} + \mathbf{K} \quad (18)$$

( $\mathbf{K}$  is a vector independent of  $y$ ). Averaging (18) over a large time interval gives an expression for the mean velocity along  $x$  (in view of two-dimensionality of mean motion,  $\bar{\alpha}_z = 0$ ,  $\alpha^{-1/2} \bar{\alpha}_z = 0$ , and there is no motion along  $z$ ):

$$U = \frac{2}{\varkappa} \overline{\alpha^{-1/2} \alpha_x} y^{1/2} + \bar{K}_x = \frac{2}{\varkappa'} (|\alpha_x| y)^{1/2} + \bar{K}_x. \quad (19)$$

Here the bar denotes an average over a long time interval:

$$\bar{\alpha}' = \bar{\alpha} \frac{(|\bar{\alpha}_x|)^{1/2}}{\alpha^{-1/2}\alpha_x}. \quad (20)$$

Expression (19) resembles the well-known “half-power law” for the separated velocity profile in a boundary layer with an adverse pressure gradient  $\bar{\alpha}_x$  [10]. However, the constant  $\bar{\alpha}'$  in (19) is not universal and, following (20), depends on the statistical regime of large-scale flow vortices which produce large-scale fluctuations of the kinematic pressure gradient. This dependence explains the observed spread of measured values in different separated and adverse pressure-gradient flows [11].

Subtracting from (18) its mean value, we determine the large-scale velocity fluctuation  $u'$ . Averaging the squares of its projections along the  $Ox$  and  $Oz$  directions, we obtain expressions for fluctuation intensities:

$$\overline{u'^2} = \frac{4}{\bar{\alpha}^2} \overline{(\alpha^{-1/2}\alpha_x - \overline{\alpha^{-1/2}\alpha_x})^2} y + O(K\alpha^{1/2}y^{1/2}); \quad (21)$$

$$\overline{w'^2} = \frac{4}{\bar{\alpha}^2} \overline{\alpha^{-1}\alpha_z^2} y + O(K\alpha^{1/2}y^{1/2}). \quad (22)$$

The values under the bar on the right-hand sides of (21) and (22) are obviously proportional to the root-mean-square fluctuation amplitude of the large-scale pressure gradient in the appropriate directions:

$$\overline{(\alpha^{-1/2}\alpha_x - \overline{\alpha^{-1/2}\alpha_x})^2} = C_x (\alpha_x'^2)^{1/2}, \quad \overline{\alpha^{-1}\alpha_z^2} = C_z (\alpha_z'^2)^{1/2}$$

where  $\alpha_x' = \alpha_x - \bar{\alpha}_x$ ;  $\alpha_z' = \alpha_z$ ; the dimensionless coefficients  $C_x$  and  $C_z$  depend on the statistical regime of fluctuations  $\alpha$ , which is determined by the structure of large-scale vortices. Hence,

$$\overline{u'^2} = \frac{4C_x}{\bar{\alpha}^2} \alpha_{x,rms}' y + o(\alpha y); \quad (23)$$

$$\overline{w'^2} = \frac{4C_z}{\bar{\alpha}^2} \alpha_{z,rms}' y + o(\alpha y). \quad (24)$$

Since large-scale velocity fluctuations are the most energetic, formulas (23) and (24) are also valid for total velocity fluctuations (including large- and small-scale fluctuations).

By virtue of the assumption of the governing role of acceleration of  $\alpha$  in the turbulence dynamics in the boundary layer of separated flow, the longitudinal spectrum of velocity fluctuations in its small-scale region, i.e., within the range of wave numbers  $\delta_N^{-1} \ll k_x \ll l_y^{-1}$ , should depend on  $\alpha$ ,  $k_x$ , and  $y$ .

For  $k_x y \ll 1$ , the statistical regime of velocity fluctuations is independent of  $y$ , and the spectrum is determined by the parameters  $\alpha$  and  $k_x$ :

$$E_{ij}(k_x) = a_{ij} \alpha k_x^{-2}, \quad \delta_N^{-1} \ll k_x \ll y^{-1}. \quad (25)$$

Here  $E_{ij}(k_x)$  is the longitudinal spectrum of velocity fluctuations:  $E_{ij}(k_x) dk_x = \overline{du_i' u_j'}$ ;  $k_x$  is the longitudinal wave number; and  $a_{ij}$  are universal constants. Expression (25) coincides with the “-2 power law” obtained for the boundary layer with an adverse pressure gradient  $\alpha$  in [12]. Averaging (25) over a long time interval, we have

$$\overline{E}_{ij}(k_x) = a_{ij}' \alpha_{rms} k_x^{-2}, \quad N^{-1} \ll k_x \ll y^{-1}, \quad (26)$$

where  $a_{ij}' = a_{ij} |\bar{\alpha}| / \alpha_{rms}$  are constants determined by the statistics of large-scale vortices;  $\alpha_{rms} = (\bar{\alpha}^2)^{1/2}$ .

In a similar way, for a small-scale spectrum of pressure fluctuations we obtain the expression  $E_{pp}(k_x) = a_p \rho^2 \alpha^2 k_x^{-3}$ , which is averaged over time to give the “-3 power law”:

$$\overline{E}_{pp}(k_x) = a_p \rho^2 \alpha_{rms}^2 k_x^{-3}. \quad (27)$$

Let us cite some experimental data confirming the above similitude laws. First let us consider the measurement results of [7] for the components of the equation of motion,

$$U \frac{\partial U}{\partial x} + V \frac{\partial U}{\partial y} + \frac{1}{\rho} \frac{\partial P}{\partial x} = \nu \left( \frac{\partial^2 U}{\partial y^2} + \frac{\partial^2 U}{\partial x^2} \right) + \frac{\partial(-\overline{u'v'})}{\partial y} - \frac{\partial \overline{u'^2}}{\partial x}, \quad (28)$$

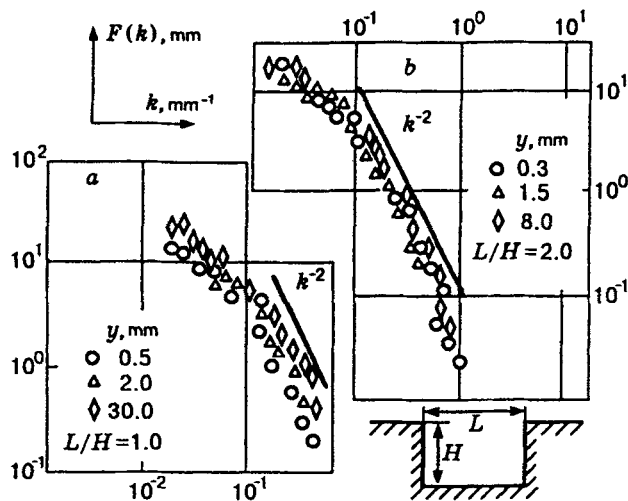


Fig. 2

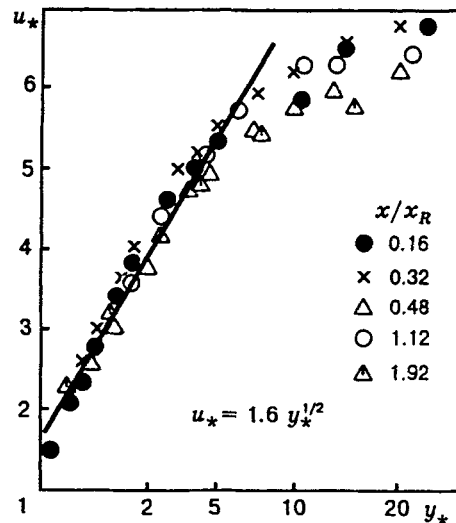


Fig. 3

in the section  $x = 397.3$  cm of the boundary layer on a flat surface downstream from the separation point. In this section, the backflow velocity has a maximum for  $N = 0.06\delta$ . As follows from the data of [7], within the near-wall layer ( $y < N$ ) convective terms are small practically everywhere. The pressure gradient constant over the section is the dominating term in Eq. (28). It is balanced by viscous accelerations in the region of  $0 < y < 0.01\delta$  and by the gradient of Reynolds shear stress in the region of  $0.01\delta < y < 0.06\delta$ . The region of  $0.01\delta < y < 0.06\delta$  can be considered a region of validity of the time-averaged relation (15). It should be noted that the data of Simpson et al. [7] do not agree with the opinion of Adams et al. [5, 6] (with reference to [7]) that terms with Reynolds stresses are insignificant in the equation of motion in the near-wall zone of recirculation flow.

Figure 2 presents longitudinal velocity fluctuation spectra  $F(k) = E_{xx}(k)/u'^2$  measured near the bottom of square (a) and rectangular (b) cavities in the middle section [13]. The square cavity was  $150 \times 150$  mm, and the thickness of the boundary layer was  $N \approx 7$  mm. As is seen from Fig. 2a, in the range of wave numbers  $k_x \gtrsim N^{-1}$  the “-2 power law” is valid in accordance with (26).

Since pressure fluctuations within the flow are difficult to measure, there are no experimental data in the literature. Let us turn to the available measurement data for pressure fluctuations on the wall. The “-3 power law” (27), which was derived above from dimensionality considerations, was previously found experimentally in [14], where Fig. 5 shows the frequency spectrum of fluctuations in different sections of the adverse pressure gradient boundary layer on a flat surface behind the separation point. When  $\omega\delta_*/U_\infty > 1$ , there is an interval  $\omega^{-3}$  in the spectrum. Following the data in [14], the phase velocity of pressure disturbances  $U_{ph}$  was constant over this frequency range within the measurement accuracy. Therefore, the data discussed can be considered a confirmation of the presence of an interval of the “-3 power law” (27) in the pressure fluctuation spectra of separated flow.

Detailed measurements of the longitudinal velocity fluctuation intensities in the near-wall layer of recirculation flow behind a sudden increase in tube diameter are presented in [6]. Figure 3 shows the data of [6] in the coordinates  $u_* = u'/v'_*$  and  $y_* = v'_*y/\nu$  ( $u'$  is the mean-square longitudinal velocity fluctuation,  $v'_* = (\tau'_w)^{1/2}$ ,  $\tau'_w$  is the root-mean-square wall shear stress fluctuation,  $x_R$  is the distance from the reattachment point). As is seen from Fig. 3, near the wall the fluctuation intensity profiles merge into one curve  $u_* = 1.6y_*^{1/2}$  in accordance with (21). It should be noted that from dimensionality considerations the “fluctuating friction velocity”  $v'_*$  should be given by the relation  $v'_* \sim (\nu\alpha_{rms})^{1/3}$ .

The smallness of the convective terms of the equation of motion in the near-wall layer of recirculation

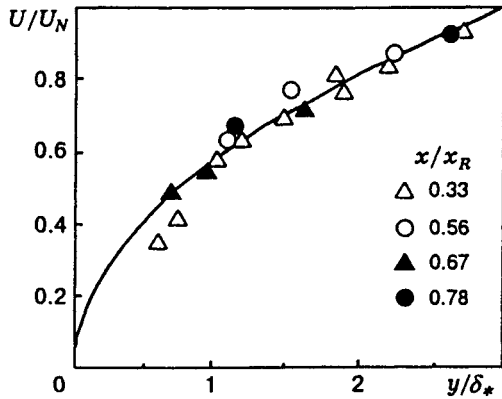


Fig. 4

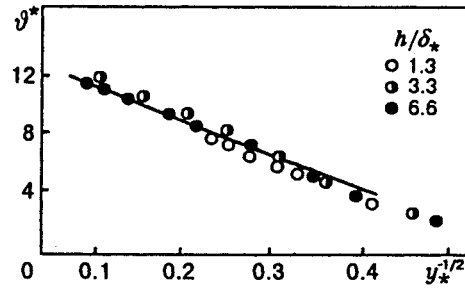


Fig. 5

flow behind the separation point, which was noted in analyzing the experimental results of [4, 7], can serve as a basis for extending the “half-power law” to the mean velocity profile (19) for the entire near-wall zone  $0 < y < N$ :

$$\frac{U}{U_N} = \left(\frac{y}{N}\right)^{1/2}.$$

The displacement thickness for such a profile is  $\delta_* = N/3$ , and hence the last relation can be written as

$$\frac{U}{U_N} = \left(\frac{y}{3\delta_*}\right)^{1/2}, \quad (29)$$

which is more convenient for comparison with an experiment, since the accuracy of experimental determination of  $N$  from the measured velocity profiles is often lower than that for  $\delta_*$ . Distribution (29) is consistent with the form parameter  $H = 2.0$ , which corresponds to the experimental value [5]. In Fig. 4, relation (29) is compared with the experimental velocity profiles in the near-wall layer of recirculation flow behind a step [5].

Thus, the assumption of the governing role of the statistical characteristics of the large-scale kinematic pressure gradient  $\alpha$  in the transfer processes in the near-wall zone of separated turbulent flow leads to the similarity laws for mean and fluctuating velocities and fluctuation spectra of velocity and pressure that are consistent with different experimental data.

**Wall Heat Transfer in Turbulent Separated Flow.** When the Prandtl numbers are on the order of unity for distances from the wall  $l_v \ll y \ll \delta_N$ , the heat transfer is characterized by a constant turbulent heat flux  $\overline{v'T'} = q/(\rho c_0)$ ,  $l_v \ll y \ll \delta_N$ . Then, the temperature gradient should be determined by the values  $q/(\rho c_0)$ ,  $\alpha$ , and  $y$ :

$$\partial T/\partial y \sim -q/(\rho c_0 \alpha^{1/2} y^{3/2}), \quad l_v \ll y \ll \delta_N,$$

which leads to an “inverse half-power law” for the temperature profile:

$$T = K_t \frac{q}{\rho c_0 (\alpha y)^{1/2}} + \text{const}$$

( $K_t$  is a universal function of the Prandtl number).

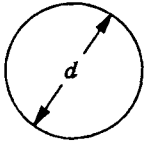
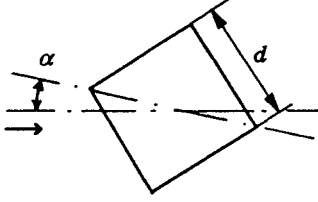
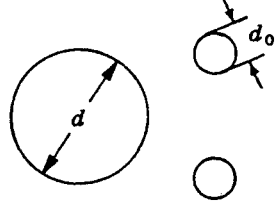
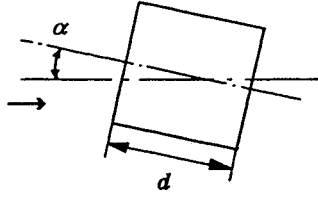
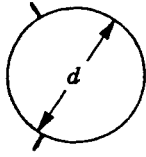
Averaging over a long time interval gives

$$\overline{T} = K'_t \frac{q}{\rho c_0 (\alpha y)^{1/2}} + \text{const}, \quad (30)$$

where

$$K'_t = K_t \frac{\alpha_{rms}^{1/2}}{\bar{q}} \left(\frac{q}{\alpha^{1/2}}\right)$$

TABLE 1

No.	Geometry	$L$	No.	Geometry	$L$
1		$d$	4		$d$
2		$d$	5		$d/\sqrt{2}$
3		$d$			

is a constant that depends on the statistical regime of large-scale vortices. Expression (30) resembles the “inverse half-power law” for the mean temperature profile in a turbulent boundary layer with an adverse pressure gradient [15].

Analysis of numerous experimental data in the literature on the temperature profiles in separated flow shows the presence of an “inverse half-power law” in the measured temperature profiles in the boundary layer. Figure 5 gives the temperature profiles in the reattachment section of separated flow behind a rectangular obstacle on a flat surface [16]. In this case,  $\vartheta^* = St^{-1/2} (T - T_w)/(T - T_\infty)$ ,  $y^* = (yU_\infty/\nu) St^{1/2}$ ,  $St = q/[\rho c_0 U_\infty (T_\infty - T_w)]$ ,  $\delta^*$  is the displacement thickness of the incoming boundary layer, and  $h$  is the obstacle height.

Following (30), with distance from the wall the temperature gradient decreases as  $y^{-1/2}$ , i.e., more rapidly than in the logarithmic distribution which is characteristic of a zero-pressure-gradient boundary layer. Therefore, the contribution of the viscous sublayer to the total thermal resistance in separated flow is more significant than in the usual turbulence boundary layer with  $dP/dx = 0$ .

Actually, from (30), one can obtain an estimate for the temperature gradient between the boundary of the viscous sublayer ( $y = l_v$ ) and the boundary of the near-wall layer ( $y = \delta_N$ ):  $\Delta T_{vN} \sim \bar{q}/[\rho c_0 (\alpha_{rms} N)^{1/2}]$ .

The temperature difference between the wall and the boundary of the viscous sublayer is of the order of  $\Delta T_{wv} \sim q l_v/\lambda$  ( $\lambda$  is the thermal conductivity). The ratio of the two values is

$$\frac{\Delta T_{vN}}{\Delta T_{wv}} \sim \frac{a}{\bar{l}_v (\alpha_{rms} N)^{1/2}}. \quad (31)$$

The thickness of the viscous sublayer in separated flow is determined from (16). Then, the thickness of the viscous sublayer  $\bar{l}_v$  averaged over a long time interval is of the order of  $\nu^{2/3} \alpha_{rms}^{-1/3}$ . Hence, expression (31) becomes

$$\frac{\Delta T_{vN}}{\Delta T_{wv}} \sim Pr^{-1} (\bar{l}_v/N)^{1/2} \ll 1.$$

Thus, one can assume that the main temperature gradient is concentrated within the viscous sublayer, in which the effective thermal conductivity is nearly molecular. Then, the wall heat transfer coefficient is



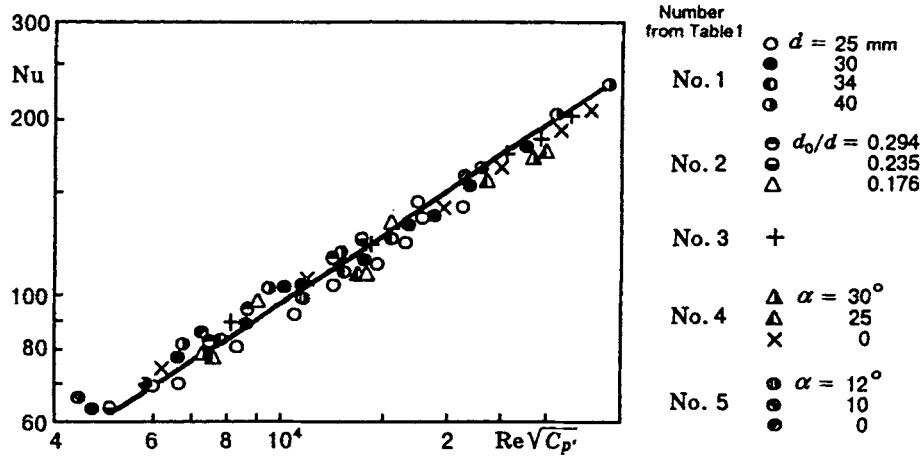


Fig. 6

given by the expression  $q/(T_w - T_\infty) \sim \lambda/l_v \sim \lambda\nu^{-2/3}\alpha^{1/3}$ , where the proportionality factor is a universal function of Pr. The average wall heat transfer coefficient is the ratio of the average thermal flux to the average temperature gradient:

$$h_w = \bar{q}/(T_w - T_\infty) = \text{const } \lambda\nu^{-2/3}\alpha_{rms}^{1/3}. \quad (32)$$

Here the proportionality factor includes, in addition to the universal function Pr, the cofactor  $\alpha^{1/3}(T_w - T_\infty)/[\alpha_{rms}^{1/3}(T_w - T_\infty)]$ , which is a coefficient that is determined by the statistics of large-scale vortices. Applying the Nusselt and Reynolds numbers  $Nu = h_w L/\lambda$  and  $Re = U_\infty L/\nu$  ( $L$  is the characteristic external dimension and  $U_\infty$  is the external flow velocity), we write (32) in the form

$$Nu = \text{const } C_\alpha^{1/3} Re^{2/3}, \quad (33)$$

where the criterion  $C_\alpha = \alpha_{rms} L/U_\infty^2$  is introduced.

The magnitude of the boundary-layer accelerations  $\alpha_{rms}$  due to large-scale vortices that move at a velocity of the order of  $U_\infty$  and have dimensions of the order of  $L$  can be estimated as  $\alpha_{rms} \sim U_\infty^2/L$ , so that the coefficient  $C_\alpha$  is independent of the Reynolds number and expression (33) is the "2/3 power law" ( $Nu \sim Re^{2/3}$ ) for turbulent heat transfer in separated flows. Thus, the "2/3 power law," which was found experimentally in the early 1960s [17] and is encountered in almost all thermal experiments with turbulent separation, has received theoretical justification for the first time.

Following (32), heat transfer intensity depends on the mean-square fluctuation amplitude of the near-wall pressure gradient  $\alpha_{rms}$ . Since no direct measurements of  $\alpha_{rms}$  have been performed, it is impossible to compare the law of heat transfer (33) with experimental data. To perform such a comparison, one should relate  $\alpha_{rms}$  to the values measured in experiments. We assume that there is a relationship between  $\alpha_{rms}$  and the level of wall pressure fluctuations  $p'_{rms}$  and the characteristic length scale of pressure disturbances  $l_p$ :

$$\alpha_{rms} = p'_{rms}/(\rho l_p). \quad (34)$$

Taking into account (34), we write (33) as

$$Nu = \text{const } (l_p/L)^{-1/3} C_p'^{1/3} Re^{2/3}, \quad (35)$$

where  $C_p' = 2p'_{rms}/(\rho U_\infty^2)$  is the coefficient of pressure fluctuations.

Expression (35) gives the relationship  $h_w \sim (p'_{rms})^{1/3}$  between the heat transfer coefficient and the

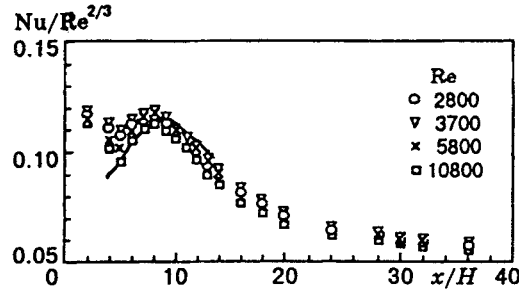


Fig. 7

level of wall pressure fluctuations obtained experimentally by Igarashi [18], who studied the effect of the fluctuation level of the bottom pressure on the average heat transfer coefficient in the rear zone of a cylinder in transverse air flow and in the rear zone of a square prism with different angles of attack. The level of pressure fluctuations in the rear zone of the cylinder were varied using a vortex generator and two parallel cylinders of smaller diameter placed across separated mixing layers (see Table 1). To compare the data of [18] with dependence (35), one should estimate the value of  $l_p$ . We assume that the length  $l_p$  is proportional to the length of the recirculation zone behind the body, which, in turn, is related to the characteristic cross-sectional dimension of the body. As the latter we can use the hydraulic diameter  $d_{\text{hydr}}$  (equal to the cylinder diameter and a square side of the prism). Assuming that the quantity  $d_{\text{hydr}}$  is the scale of  $L$  in the  $Nu$  and  $Re$  numbers and setting  $l_p \sim d_{\text{hydr}} = L$ , we obtain, in accordance with (35),  $Nu \sim C_p^{1/3} Re^{2/3}$ . As is seen from Fig. 6, the experimental data of [12] are generalized by the dependence (curve)

$$Nu = 0.21 C_p^{1/3} Re^{2/3}. \quad (36)$$

For a blunt face of the prism (see Table 1, No. 5) it is assumed that  $L = d_{\text{hydr}}/\sqrt{2}$ , since its cross-sectional dimensions are smaller by a factor of  $\sqrt{2}$  compared with a sharp edge of the prism (No. 4).

The local heat transfer on the surface of a flat plate in air flow was studied by Ota [19]. Similar studies of the hydrodynamics of this object were carried out Kiya et al. [20, 21]. Cherry [21] measured the pressure-fluctuation distribution on the wall. Let us assume that the scale  $l_p$  is constant and proportional to the half-width of the plate  $H$  and set  $L = H$ . Then, expression (35) yields  $Nu \sim C_p^{1/3} Re^{2/3}$ . Figure 7 presents the data of [19] on the distribution of  $NuRe^{-2/3}$  over the plate surface compared with the dependence (curve)

$$NuRe^{-2/3} = 0.23 C_p^{1/3}, \quad (37)$$

which describes well the experimental data, except for the region near the leading edge. In this region, in view of the proximity of the shedding mixing layer, the turbulence scale is proportional to  $x$  [20, 21]. A corresponding decrease in the scale  $l_p$  leads, according to (35), to an increase in the heat transfer coefficient. Note the similarity of (36) and (37).

The influence of the Prandtl number on the heat transfer coefficient is usually taken into account by including the function  $Pr^\beta$  in the dependence for heat transfer. Following the recommendations in [22] based on measurements of heat transfer in the cylinder's rear zone for  $0.7 < Pr < 100$ , it is assumed that the exponent  $\beta$  is 0.45, so that the laws of heat transfer for the cylinder and plate, respectively, take the form

$$Nu = 0.25 C_p^{1/3} Re^{2/3} Pr^{0.45}, \quad Nu = 0.27 C_p^{1/3} Re^{2/3} Pr^{0.45}.$$

Thus, the laws obtained for transfer processes are supported by experimental results. The model proposed can be considered a basis for constructing acceptable wall functions, which are necessary for hydrodynamics and heat-and-mass-transfer calculations in complex turbulent flows with separation.

## REFERENCES

1. B. E. Launder, "On the computation of convective heat transfer in complex turbulent flows," *Trans. ASME, Ser. C, J. Heat Transfer*, No. 4, 1112 (1988).
2. E. M. Khabakhpasheva and G. I. Efimenko, "Structure of turbulent flow in a plane diffuser," in: *Structure of Forced and Thermogravitational Flows* [in Russian], Institute of Thermophysics, Sib. Div., Russian Acad. of Sci., Novosibirsk (1983), pp. 5-31.
3. Y. Nagano, M. Tagawa, and D. Tsuji, "Effects of adverse pressure gradient on mean flows and turbulence statistics in a boundary layer," in: *Turbulent Shear Flows 8, Selected Papers from the 8th International Symposium, Munich* (1993), pp. 7-21.
4. R. L. Simpson, "Turbulent boundary-layer separation," *Ann. Rev. Fluid Mech.*, **21**, 205-234 (1989).
5. E. V. Adams and J. P. Johnston, "Flow structure in a boundary layer of a turbulent separated flow," *Aerocosh. Tekh.*, No. 5, 3-13 (1989).
6. W. J. Devenport and E. P. Sutton, "Near-wall behavior of separated and reattaching flows," *AIAA J.*, **29**, No. 1, 25-31 (1991).
7. R. L. Simpson, Y. T. Chew, and B. G. Shivaprasad, "Structure of a separating turbulent boundary layer. Part 1. Mean flow and Reynolds stresses. Part 2. Higher-order turbulence results," *J. Fluid Mech.*, **113**, 23-51 and 53-73 (1981).
8. H. Tennekes and J. L. Lumley, *A First Course in Turbulence*, MIT Press, Cambridge, Mass. (1972).
9. H. S. Govinda Ram and V. H. Arakeri, "Studies on unsteady pressure field in the region of separating or reattaching flows," *J. Fluid Eng.*, **112**, 402-408 (1990).
10. A. A. Townsend, *The Structure of Turbulent Shear Flow*, Cambridge Univ. Press, Cambridge (1976).
11. A. E. Perry and W. H. Schofield, "Mean velocity and shear stress distribution in turbulent boundary layers," *Phys. Fluids*, **16**, No. 12, 2068-2074 (1973).
12. B. A. Kader and A. M. Yaglom, "Spectra of anisotropic turbulent pulsations of velocity and temperature in near-wall turbulent flows," in: *Problems of Turbulent Flows* [Russian translation], Nauka, Moscow (1987), pp. 65-74.
13. I. M. Varfolomeev, G. A. Glebov, Yu. F. Gortyshov, et al., "Structure of turbulent separated flow in a rectangular cavity," in: *Near-Wall Jet Flows* [in Russian], E. P. Volchkov (ed.), Inst. Thermal Phys., Sib. Div, Russian Acad. Sci., Novosibirsk (1984), pp. 86-92.
14. R. L. Simpson, M. Ghodbane, and B. E. McGrath, "Surface pressure fluctuations in a separating turbulent boundary layer," *J. Fluid Mech.*, **177**, 167-186 (1987).
15. B. A. Kader, "Heat and mass transfer in pressure-gradient boundary layers," *Int. J. Heat Mass Transfer*, **34**, No. 11, 2837-2858 (1991).
16. A. Pedishyus and A. Shlanciauskas, *Near-Wall Turbulent Heat Transfer* [in Russian], Mokslas, Vilnius (1987).
17. Paul K. Chang, *Separation of Flows*, Pergamon Press, Oxford (1970).
18. T. Igarashi, "Correlation between heat transfer and fluctuating pressure in the separated region of a bluff body," in: *8th Int. Heat Transfer Conf.*, San Francisco, **3** (1986), pp. 1023-1028.
19. T. Ota and N. Kon, "Heat transfer in separated and reattaching flows on a blunt flat plate," *Trans. ASME, Ser. C, J. Heat Transfer*, **96**, No. 4, 29-32 (1974).
20. M. Kija and K. Sasaki, "Structure of a turbulent separation bubble," *J. Fluid Mech.*, **137**, 83-113 (1983).
21. N. J. Cherry, R. Hillier, and M. E. M. P. Latour, "Unsteady measurements in a separated and reattaching flow," *J. Fluid Mech.*, **144**, 13-46 (1984).
22. A. Zhukauskas and I. Zhyugzhda, *Heat Release of a Cylinder in Transverse Liquid Flow* [in Russian], Mokslas, Vilnius (1979).